JOURNAL OF APPLIED ELECTROCHEMISTRY **29** (1999) 361–369.

Studies on metal hydride electrodes with different weights and binder contents

G. ZHENG, B. S. HARAN, B. N. POPOV *, R. E. WHITE

Department of Chemical Engineering, University of South Carolina, Columbia, SC 29208, USA
*(*author for correspondence, e-mail: popov@engr.sc.edu)*

Received 10 January 1998; revised 15 May 1998

$LaNi_{4.27}Sn_{0.24}$ electrodes were characterized using electrochemical techniques at different alloy weights and binder contents. For a given alloy weight, the polarization resistance (R_p) increases with the state of charge (SOC). This arises due to changes from α to β phase at the alloy surface. The electroactive surface area for the hydrogen adsorption/desorption reaction changes with SOC and this also contributes to the variation of R_p. Since the interfacial area increases with alloy content, the polarization resistance decreases with increase in the alloy weight. An increase in the alloy weight reduces R_p and lowers the total resistance. The electrode utilization decreases by increasing the binder content and the electrode weight. A theoretical model is presented to study the effect of alloy weight and particle size on the electrode performance. The model simulations predict lowering of the utilization with increase in the electrode weight. The effect of particle size on the energy and power density of the electrode was also studied.

Keywords: *metal-hydrides*, *alloy weight*, *binder content*, *electrochemical impedance spectroscopy*, *model simulations*

List of symbols

a_{MH}	electroactive surface area per unit volume of electrode ($cm^2\ cm^{-3}$)
A	cross-sectional area of the pellet electrode (cm^2)
c°	reference hydrogen concentration (mol cm^{-3})
$\hat{c}$	dimensionless hydrogen concentration (c/c°)
$\hat{c}_s$	dimensionless surface concentration of hydrogen
d	density of the alloy (g cm^{-3})
D	diffusion coefficient of hydrogen ($cm^2\ s^{-1}$)
F	Faraday's constant (96 487 C mol^{-1})
j	specific discharge current (A g^{-1})
j'	local current density (A cm^{-2})
j_o	exchange current density per unit mass of alloy (A g^{-1})
Q_o	specific capacity of the electrode (Ah g^{-1})
$\hat{r}$	dimensionless radial coordinate (r/R_s)
R_s	radius of the metal hydride particles (cm)
R_p	polarization resistance (Ω g)
R	universal gas constant (8.314 J $mol^{-1}\ K^{-1}$)
T	temperature (K)
t	thickness of the pellet (cm)
t_{cc}	thickness of the current collector (cm)
U	electrode utilization
V	volume of the cylindrical pellet electrode (cm^{-3})
w	amount of active material (g)

Greek symbols

δ	dimensionless parameter denoting ratio between diffusional and kinetic resistances, $j' R_s/Fc^\circ D$
ε	porosity of the electrode
η	overpotential (V)
τ	dimensionless time
τ_D	dimensionless time to completely discharge the electrode

1. Introduction

Metal hydrides form a class of solid-state systems called interstitial alloys wherein hydrogen is incorporated into empty sites of a simple metal lattice [1]. For practical electrochemical devices, metal hydrides are sought with the following properties: high capacity to store hydrogen, low hydrogen equilibrium pressure, fast kinetics, low cost and light weight [1–5]. Significant studies have been done in identifying alloys with low equilibrium pressure and stability. However, very few investigations have been reported in the literature on the determination of the electrochemical parameters such as the polarization resistance, exchange current density and electrode utilization [2, 3, 6–10]. Determination of the electrochemical parameters is essential for optimizing the alloy performance.

Previous studies [9, 10] have focussed on determining the different electrode thermodynamic and kinetic parameters as a function of state of charge. We have shown, by applying porous electrode theory [2, 3], that one can calculate the exchange current density of the alloy at low overpotentials. The exchange current density is a measure of the electrocatalytic activity of the hydride alloy. With poor

reaction rates, the polarization resistance is high, which significantly reduces the energy and power density of the battery. Although the composition of the alloy affects the exchange current, and thereby the reactions rate, it can be modified by microencapsulation or chemical treatment of the surface. However, according to Kuriyama *et al.* [4] only one third of the total hydride electrode resistance was due to the polarization resistance. For practical applications, apart from the kinetic resistance, different ohmic resistances in the electrode are also significant. The performance under high discharge currents is more dependent on the electrode size and morphology.

For an electrode of given geometry the thickness and the alloy weight significantly alter the discharge characteristics. Zuettel, Meli and Schlapbach [11] investigated the influence of the electrode thickness on the overpotential during charge and discharge. The overpotential was found to depend on the discharge time and the thickness of the electrode. Apart from the size and porosity of the electrodes, another parameter, which alters the resistance, is the kind and amount of binder material. Fabrication of hydride electrodes involves the addition of small amounts of binder, which keeps the particles intact and enhances the mechanical stability of the electrode. Apart from binders such as PTFE, the alloy is also mixed with different conductive powders. Studies have been made on compacting electrodes with different metal oxides such as Co_3O_4 and RuO_2 and also different diluents such as metal powders of Ni, Cu and Co. For an alloy of given composition the binder and various diluents change the electrode performance by affecting the capacity and cycle life. Therefore, it is of interest to characterize the electrode parameters as a function of both the electrode size and the binder content. Since PTFE is a commonly used binder the present study was to focus on its effect in isolation without any other additions.

In this work linear polarization and electrochemical impedance spectroscopy (EIS) were used to carry out a detailed study on the determination of the electrochemical properties of $LaNi_{4.27}Sn_{0.24}$ as a function of the electrode weight and the binder content. Studies on the binder content were focussed solely on the effect of PTFE addition. Different resistances of the alloy electrode were evaluated by fitting the EIS data to an equivalent circuit as suggested by Kuriyama *et al.* [4]. The performance of the electrode was analysed using a simple analytical model. The effect of different alloy weights and particle sizes was also studied.

2. Model

The electrode reaction at the surface of the hydride particle is

$$MH_{x,ads} + x\,OH^- \underset{\text{charge}}{\overset{\text{discharge}}{\longleftrightarrow}} M + x\,H_2O + x\,e^- \quad \text{(I)}$$

To determine the surface hydrogen concentration for a galvanostatic charge/discharge, the concentration profile of hydrogen has been obtained [12] by solving the time-dependent Fickian diffusion equation for the spherical particle in dimensionless form,

$$\frac{\partial \hat{c}}{\partial \tau} = \frac{1}{\hat{r}^2}\frac{\partial}{\partial \hat{r}}\left(\hat{r}^2 \frac{\partial \hat{c}}{\partial \hat{r}}\right) \tag{1}$$

The initial and boundary conditions are

$$\text{at} \quad \tau = 0, \quad \hat{c} = 1 \tag{2}$$

$$\text{at} \quad \hat{r} = 0, \quad \frac{\partial \hat{c}}{\partial \hat{r}} = 0 \tag{3}$$

$$\text{at} \quad \hat{r} = 1, \quad \frac{\partial \hat{c}}{\partial \hat{r}} = -\frac{j' R_s}{FDc^\circ} \tag{4}$$

The local current density, j', represents the reaction rate at the particle/solution interface and is given by

$$j' = \frac{jw}{a_{MH} V(1-\varepsilon)} \tag{5}$$

where the electroactive surface area, a_{MH} is given by

$$a_{MH} = \frac{3(1-\varepsilon)}{R_s} \tag{6}$$

and the volume of the pellet is given by

$$V = At \tag{7}$$

where A and t are the cross-sectional area and thickness of the pellet, respectively. The thickness of the pellet is calculated as

$$t = \frac{w}{Ad} + t_{cc} \tag{8}$$

where d is the density of the alloy and t_{cc} is the thickness of the current collector. Solving Equation 1 subject to initial and boundary conditions Equations 2 to 4 gives the concentration as a function of time and radial coordinate. For a constant current discharge the variable of interest, namely the dimensionless surface concentration ($\hat{c}_s$) is obtained as

$$\hat{c}_s = 1 - \delta\left[3\tau + 0.2 - 2\sum_{n=1}^{\infty}\frac{1}{\lambda_n^2}\exp\left(-\lambda_n^2\tau\right)\right] \tag{9}$$

where, δ a dimensionless parameter, is given by

$$\delta = \frac{j' R_s}{Fc^\circ D} \tag{10}$$

Equation 9 can be rewritten to calculate the time for discharge, τ_d, for the metal hydride electrode when the surface concentration drops to zero,

$$\delta = \frac{1}{\left[3\tau_D + 0.2 - 2\sum_{n=1}^{\infty}\frac{1}{\lambda_n^2}\exp\left(-\lambda_n^2\tau_d\right)\right]} \tag{11}$$

For a given current per unit mass, j, Equation 11 can be solved to obtain the time for discharge, τ_d. For long discharge periods the discharge time can be directly obtained as

$$\tau_D = \left(\frac{1}{\delta} - 0.2\right) \times \frac{1}{3} \tag{12}$$

The electrode utilization is then calculated as

$$U = \frac{jt_D R_s^2}{3600\,Q_o D} \times 100\% \tag{13}$$

Table 1. Parameters used in the simulation

Properties	*Values*	*Reference*
Diffusion coefficient of hydrogen (D)	$6.75 \times 10^{-11}\,cm^2\,s^{-1}$	measured
Density of the alloy (d)	$7.8\,g\,cm^{-3}$	assumed
Pellet electrode area (V)	$0.5\,cm^2$	measured
Thickness of the current collectors	0.005 cm	measured
Electrode capacity (Q_o)	$270\,mAh\,g^{-1}$	measured
Particle radius (R_s)	15 μm	measured
Porosity (ε)	0.4	measured
Reference hydrogen concentration (c^o)	$91.3\,mol\,cm^{-3}$	[1]

where Q_o is the actual specific capacity of the electrode. The model does not consider ohmic resistance and both solid and solution phase conductivities are assumed to be large compared to diffusional resistance. The parameters used in the simulation are given in Table 1.

3. Experimental details

The alloy $LaNi_{4.27}Sn_{0.24}$ was first crushed and ground mechanically. The resulting powder was passed through a 230 mesh sieve, which gave a particle size of less than 63 μm. A rough estimate of the porosity of the alloy was obtained by saturating a known weight of the alloy in KOH solution and determining the volume. Next, pellet electrodes were prepared by mixing the alloy with PTFE powder and then pressing the material in a cylindrical press (8 mm dia.) between two nickel meshes at 150 to 200 °C. For the studies on electrodes with different weights, pellets with alloy weights of 0.10, 0.20, 0.32 and 0.65 g were prepared. The cross-sectional area of all the electrodes is 0.5 cm^2. The PTFE content was kept at 5% of alloy weight for these pellets. For studies on binder content, different pellet electrodes with 2.5, 5, 10, 20 and 40% PTFE mixed with a constant alloy weight of 0.2 g were prepared. The pellet was then inserted between two pieces of plexiglass with small holes on each side. A piece of Pt gauze was placed on each side of the plexiglass and served as the counter electrode. The electrode was immersed in the test cell and filled with 6 M KOH electrolyte solution. The experiments were carried out using Hg/HgO reference electrode. A schematic of the experimental setup is shown in Fig. 1.

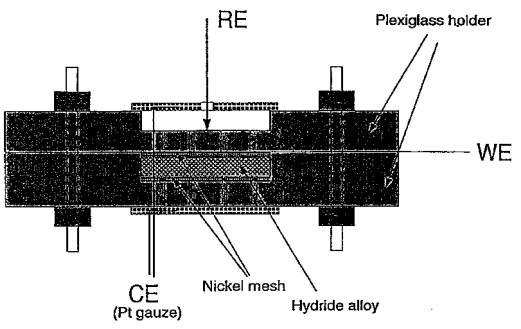

Fig. 1. Schematic of pellet electrode.

Prior to each experiment, the alloy electrode was activated by cycling the electrode ten times. The experimental procedure was performed as follows. The electrode was charged under a constant current mode until the hydrogen content reached its saturated value. Before conducting any experiments sufficient amount of time (1 h) was allowed for the potential to stabilize. The electrode was gently shaken to remove any hydrogen bubbles that could have formed. After the open circuit potential (OCP) stabilized, linear polarization and EIS experiments were carried out. The electrode was discharged at 0.1 C rate for a certain period of time and the same measurements as above were conducted. This procedure was repeated until the electrode was totally discharged to a cut-off voltage of −0.6 V. Impedance studies covered a frequency range from 100 kHz to 1 mHz and involved a total time of approximately 1 h. The electrode potential changed by less than 2 mV during this time indicating that self-discharge processes were not significant. Polarization studies were done at a scan rate of 1 mV s^{-1} by sweeping the potential 20 mV above and below the equilibrium potential. Since the scan rate was kept low and the potential was not perturbed to large anodic values the concentration of hydrogen at the surface does not change significantly. The electrode can be assumed to be at pseudo steady state and the linearized form of the Butler–Volmer equation can be used to determine the exchange current density. Altering any of the two conditions mentioned above would lead to a varying surface hydrogen concentration and invalidate this approximation. The experiments were conducted at 25 °C using the SoftCorr system (model 342C) with EG&G PAR potentiostat/galvanostat (model 273A).

4. Results and discussion

4.1. *Characterization of metal hydride electrodes with different alloy weights*

Studies on $LaNi_{4.27}Sn_{0.24}$ have been carried out using electrodes with different thickness. Four pellets were prepared with different alloy weights (0.10, 0.20, 0.32 and 0.65 g) which had the same diameter. The linear current response was measured for a small potential perturbation of 20 mV about the equilibrium potential. Beyond these potentials, hydrogen transport in the alloy becomes significant and concentration polarization rather than activation overpotential controls the current response of the electrode. Typical linear polarization curves for fully charged electrodes with different alloy weights are presented in Fig. 2. In the polarization studies since the deviation in potential is small, the change in the SOC of the electrode is less than 1%. In such a case the mass transfer effects arising due to the hydrogen transport in the particle can be neglected and the overpotential associated with any given current serves solely as an activation energy. In our previous studies applying porous electrode theory [2, 3] it was found that a low over-

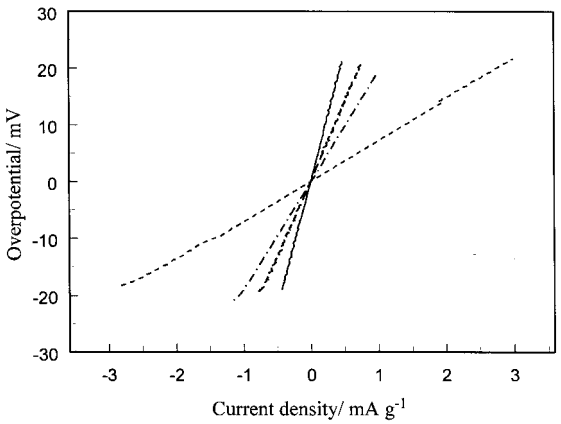

Fig. 2. Polarization curves obtained at different alloy weights for fully charged electrodes. The potential was perturbed 20 mV above and below the steady state equilibrium potential for all weights. Scan rate 1 mV s^{-1}; 2.5% PTFE content. Key: (——) 0.10, (– – – –) 0.20, (—·—) 0.32 and (- - - - -) 0.65 g.

potentials the exchange current density, j_o, of the alloy could be calculated using Equation 14

$$j_o = \frac{RT}{FR_p} \tag{14}$$

where R is the gas constant, F is the Faraday's constant, T is the temperature and R_p is the polarization resistance.

The total resistance (R_t) was determined from the slope of each curve. As shown in Fig. 2, the slopes increase with the decrease of the alloy weight. The total resistance determined from the slopes in Fig. 2 is presented in Fig. 3 as a function of state of charge (SOC). At high SOC, the total resistance is inversely proportional to the electrode weight, while as shown in Fig. 3, at low SOC (SOC $< 50\%$), the total resistance is virtually independent of the electrode weight. At low electrode weight the total resistance varied significantly with the state of charge (SOC). However, at higher electrode weights this effect was less pronounced. At an alloy weight of 0.65 g, the total resistance was almost independent of the state of charge. The results presented in Fig. 3 may be explained qualitatively by taking into account the contribution of the polarization resistance and the ohmic resistance of the alloy to the total resistance. The polarization resistance is inversely proportional to the alloy weight, while as found by Kuriyama *et al.* [4] the electrode ohmic resistance is independent of the alloy weight. Thus, the observed dependence in Fig. 3 of the total resistance on the alloy weight indicates that at a high SOC, the polarization resistance dominates the total resistance. As the hydrogen content in the alloy decreases (low SOC) the resistance to charge transfer also decreases. At a high SOC, the hydrogen reaction occurs on the metal–hydride surface instead on the bare alloy causing the reactivity of the hydrogen reaction to decrease when compared with hydrogen evolution reaction on the bare alloy surface. During hydriding AB_5 alloys change from the α phase (hydrogen deficient) to the β phase (hydrogen rich). The polarization resistance is governed by the behaviour of the alloy/electrolyte interface. At the surface initially the alloy is in the α phase (hydrogen deficient). Only at the end of charge the entire particle is in the β phase. During most of the hydriding the alloy is present in both the α and β phases. Since the resistance depends on the α–β transitions, it changes significantly beyond 90% SOC, where the alloy is in the β phase. Increase in alloy weight increases the active surface area and reduces the total resistance. Thus, both the alloy weight and hydrogen content are factors which affect the value of the polarization resistance. The SOC studies were repeated and similar results were obtained. Metal hydrides are highly reversible to hydrogen and results obtained are easily reproducible.

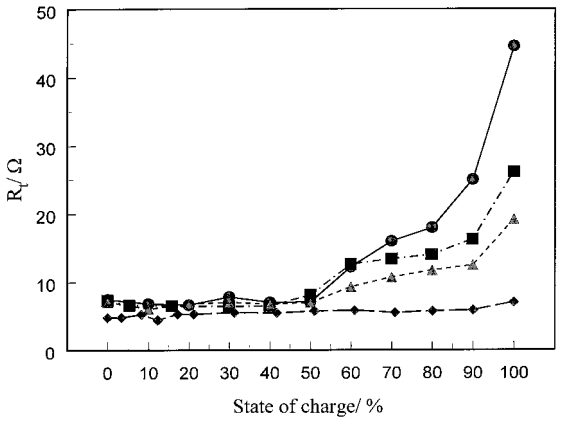

Fig. 3. Total electrode resistance as a function of state of charge for different alloy weights with 2.5% PTFE. Key: (●) 0.10, (■) 0.20, (▲) 0.32 and (◆) 0.65 g.

Electrochemical impedance spectroscopy (EIS) under zero current conditions enables the determination of the polarization resistance and evaluation of the exchange current density without the interference of any of the ohmic resistance (related to alloy particle to particle resistance and contact resistance between the current collector and the pellet). According to Kuriyama *et al.* [4–6] the total resistance of the system is a sum of the following resistances: (i) the electrolyte resistance, (ii) the resistance between the current collector and the electrode pellet, (iii) the alloy particle to particle contact resistance and (iv) the polarization resistance which is related to the electrode reaction on the alloy surface and is inversely proportional to the active surface area.

Typical Nyquist plots obtained for different alloy weights at 100% state of charge are presented in Fig. 4. The total resistances measured from both techniques agree within 1% for different SOC values. The Nyquist plots indicate that the total impedance increases with a decrease of the alloy weight, which is consistent with the linear polarization results. The semicircle observed at low frequency corresponds to the faradaic contribution while the semicircle observed at high frequency corresponds to the ohmic resistance. Further, the two semicircles shown in Fig. 4 are most distinguishable at large alloy weights,

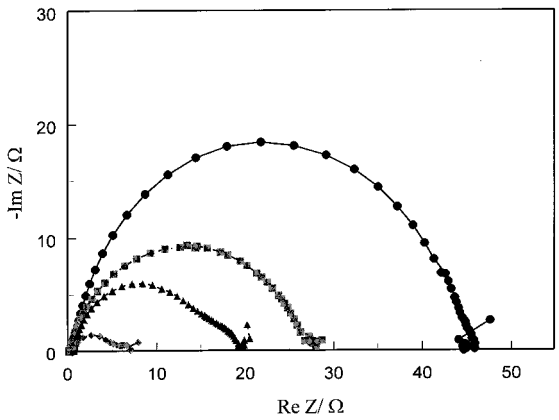

Fig. 4. Nyquist plots for different alloy weights at 100% state of charge with 2.5% PTFE. Key: (●) 0.10, (■) 0.20, (▲) 0.32 and (◆) 0.65 g.

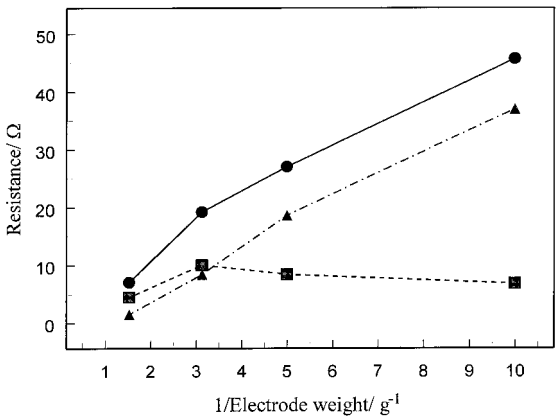

Fig. 6. Various electrode resistances as a function of inverse alloy weight for fully charged electrodes with 2.5% PTFE. Key: (●) R_t, (■) R_o and (▲) R_p.

that is, at 0.65 g of alloy weight. For the metal hydride electrodes with low alloy weights, the faradaic resistance dominates over the ohmic resistance and only one semicircle is observed in the Nyquist plot. The ohmic resistance remains the same at different alloy weights. However, the polarization resistance masks the effect of ohmic resistance at low alloy weights. Increasing the alloy weight increases the electroactive surface area, thereby reducing R_p. Hence, for the electrodes which contain a large amount of alloy (0.65 g), the ohmic resistance (the semicircle at high frequency) is comparable with the polarization resistance causing both semicircles (as shown in Fig. 4) to be visible. In our case, increasing the weight of the electrode also result in increasing the pellet thickness. However, from a design point of view thicker electrodes are undesirable for high load applications such as electric vehicles. This would be seen clearly from the model simulations shown later in this paper.

The equivalent circuit shown in Fig. 5 was used to fit the experimental impedance data. R_{el} represents the electrolyte resistance, R_{cp} is the current collector to pellet resistance, R_{pp} is the particle to particle resistance, R_p is the polarization resistance, R_w is the Warburg resistance, C's are the capacitances and Q_{cpe}'s are the constant phase elements (CPE) [12].

The experiment results shown in Fig. 4 were fitted by using Zview (Scribner Associates, Inc.). The resistances estimated from the fitting are plotted in Fig. 6 as a function of the inverse of the alloy weight. As shown in this plot, the polarization resistance is inversely proportional to the alloy weight. However, the ohmic resistance, R_o, (the sum of particle to particle contact resistance and current collector to pellet contact resistance) remains independent of the alloy weight. A linear decrease of the polarization resistance and hence of the total resistance is seen on increasing the alloy weight. This lowering of R_p arises due to an increase in the electroactive surface area available for Reaction I. The intercalation of hydrogen in these alloys proceeds with the reaction at the interface of the particle and electrolyte. Increase in the interfacial area facilitates the reaction to proceed on more sites thereby reducing both R_p and R_t. Not accounting for this increase in area would give erroneous results when calculating the exchange current for Reaction I. Conventionally, the exchange current has been normalized by dividing it by the electrode area to get an effective equilibrium current density. However, metal hydride electrodes are porous in nature and determination of electrode surface area in such cases is complicated. Further, as seen in Fig. 3 the active surface area changes with SOC, which cannot be measured experimentally. Hence we normalized our exchange current density based on the total alloy weight in the electrode. The linear change in the polarization resistance with alloy weights supports this approach. Finally, the exchange current density (for the electrode, which contained 0.65 g of alloy weight,) was estimated from the polarization resistance in Fig. 6 to be 17 mA g^{-1} compared with a value of 3.6 mA g^{-1} estimated from the total resistance.

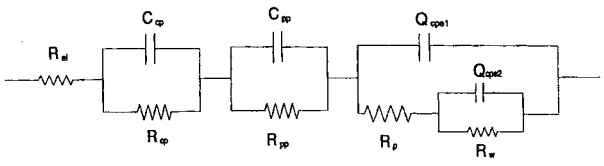

Fig. 5. Schematic of the equivalent circuit for the metal hydride electrode.

Figure 7 shows the fitting results obtained for the polarization, ohmic and total resistances of 0.2 g alloy plotted as a function of state of charge. As shown in this plot, the polarization resistance decreases with a decrease of SOC. At a SOC lower than 40%, the polarization resistance is almost constant. As discussed before, changes in the electroactive surface area vary the reaction resistance with SOC. The ohmic resistance remains independent of the SOC. The ohmic resistance changes only due to variations in the electrolyte and matrix phase conductivity. The electrolyte conductivity is affected by changes in the concentration of the hydroxide ion. After hundreds of cycles the electrolyte is depleted of OH^- and the conductivity is

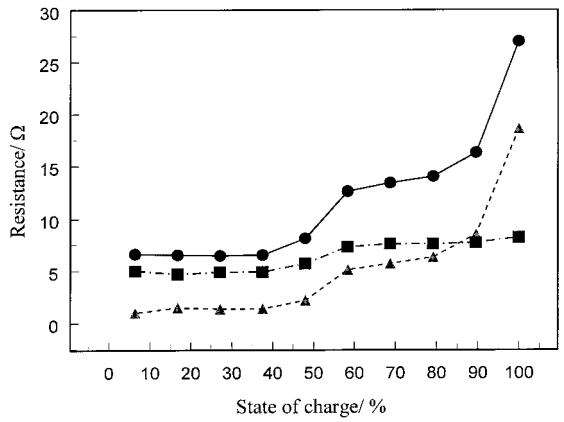

Fig. 7. Change in different electrode resistances as a function of state of charge. Key: (●) R_t, (▲) R_p and (■) R_o.

lower. At low discharge rates, in any particular discharge cycle concentration variations in KOH are not significant enough to affect the electrolyte conductivity. Similarly, the matrix phase conductivity is not affected by the intercalation of hydrogen. However, the particle–particle resistance increases with cycling because of loss of contact among different particles in the solid matrix. In such a scenario, the role of different binders becomes crucial.

4.2. *Characterization of metal hydride electrodes with different percentage of binder*

Various binders and additives have been proposed in the literature for improved performance of hydride alloys. However, PTFE remains the most common of all the additives used in the preparation of hydride cells. Hence we focussed our studies on the effect of various amounts of PTFE on the performance of the hydride electrode for a given amount of alloy weight. The objective was to arrive at an optimized value of PTFE content for use in the preparation of electrodes. The experiments were conducted at five different binder (PTFE) contents (2.5, 5, 10, 20 and 40%) using 0.2 g of alloy weight. Figure 8 shows the Nyquist plots obtained for different percentages of PTFE content in the alloy for a fully charged electrode. As shown in this plot, the minimum resistance was observed at a PTFE content of about 5%. Increasing the PTFE content in the alloy beyond 5% causes the resistance to increase drastically. This phenomenon can be explained by considering that at smaller percentage of the binder (PTFE), the contact resistance between the alloy particles is high. On increasing the PTFE content to 5%, the ohmic resistance becomes smaller due to a better contact among the particles. When PTFE content is higher, the total alloy in the electrode is lower. Further at high concentrations, PTFE acts as an insulator thereby increasing the contact resistance.

By fitting the experimental data given in Fig. 8 using the equivalent circuit presented in Fig. 5, the polarization resistance and ohmic resistance were evalutated and are presented in Fig. 9. As shown in this plot, both the total resistance and the ohmic resistance have a minimum at a PTFE of 5% and as expected both resistances increase by increasing the PTFE content in the alloy. As shown in Fig. 9, the polarization resistance is independent of the PTFE content beyond 2.5%. For 2.5% PTFE, not all the particles are in contact with each other and hence the active surface area is less. Due to this the polarization resistance is larger compared to other PTFE values given. Beyond this PTFE content all the particles are in contact. Hence, R_p remains the same. Since the amount of alloy was kept constant at 0.2 g, the electroactive surface area remains the same in all these studies. Hence, the polarization resistance remains constant and does not vary with binder content.

Figure 10 represents the electrode utilization as a function of PTFE content in the alloy. As shown in this plot, the electrode utilization decreases by increasing the PTFE content from 5% up to 20% of the active material of the electrode. Maximum utilization of the electrode was observed at 5% PTFE, which is consistent with the results presented in Fig. 9. Increasing the PTFE content in the alloy, causes the total resistance (as shown in Fig. 9) to increase which results in a decrease of the electrode utilization. From

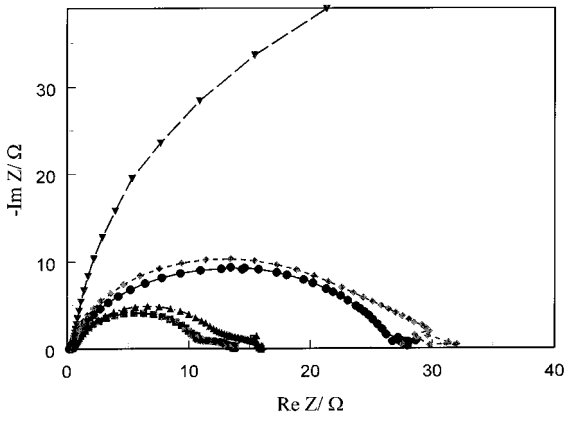

Fig. 8. Nyquist plots for different PTFE contents at 100% state of charge. The alloy weight is 0.2 g. Key: (●) 2.5%, (■) 5.0%, (▲) 10.0%; (◆) 20.0% and (▼) 40.0%.

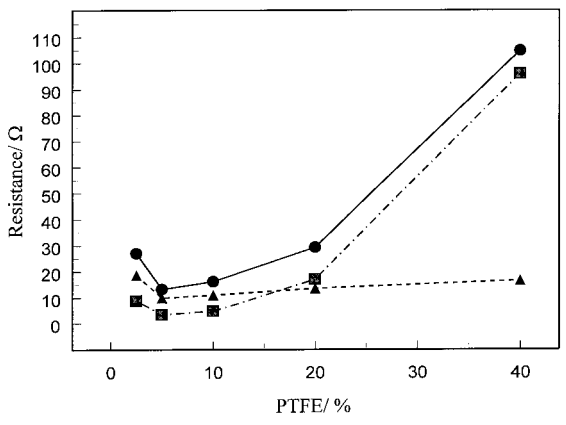

Fig. 9. Different electrode resistances as a function of PTFE content for fully charged electrodes for 0.2 g of alloy. Key: (●) R_t, (■) R_o and (▲) R_p.

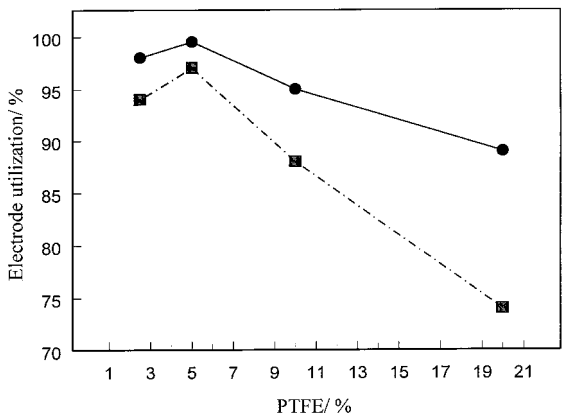

Fig. 10. Electrode utilization as a function of PTFE content at two different discharge rates for 0.2 g of alloy. Key: (●) 0.1 *C* and (■) 0.2 *C*.

these studies we have arrived at an optimized value of the binder content, namely 5%.

4.3. *Simulation results*

Figure 11 presents the discharge time as calculated by Equation 12 for different specific currents. At the end of discharge when the electrode reaches it's cut-off potential the hydrogen concentration at the surface of the particle is close to zero. The time for hydrogen concentration to drop to zero depends on the applied current. As seen from Fig. 11, the time for discharge decreases with an increase in the applied specific current. The discharge of the metal hydride electrode is controlled by the transport of active species both inside and outside the particle [12]. Mass transfer limitations in the hydride electrode arise due to the transport of hydrogen in the particle and the movement of hydroxide ions in the solution. Increase in discharge currents would result in depleting the surface hydrogen faster, although enough amount of hydrogen is present in particle. However, at high rates external mass transfer effects due to hydroxide ion transport limitations also become significant. The exponential decay in the discharge time would be more pronounced if concentration polarization in the solid and electrolyte were also considered. Further, the time for discharge decreases with an increase in the electrode weight. Increase in the electrode weight would result in increasing the concentration polarization significantly. This would also cause the discharge time to be smaller.

An important parameter that defines the performance of the alloy as an electrode is utilization. The electrode utilization is defined as the ratio of the hydrogen discharged at a specific rate to the maximum experimental capacity of the same electrode. The electrode utilization for small currents is obtained by substituting the expression for the discharge time from Equation 12 into Equation 13. Utilization estimated at two different discharge rates (0.1 *C* and 0.2 *C*), is plotted as a function of the alloy weight of the electrode in Fig. 12. The simulations from Equation 13 are also given in the same plot. The utilization is related to the electrode weight through δ which includes the parameters, current and volume, both of which depend on the alloy weight. As shown in Fig. 12, the electrode utilization decreases by increasing the alloy weight of the electrode. Consequently, at low alloy weights, the discharge rate depends only on the hydrogen diffusion in the solid phase. This results in values of the electrode utilization close to 100%. Increasing the electrode weight has the effect of increasing the electrode thickness. In such cases, concentration polarization starts to play a more important role in the current potential relationship and the electrode utilization is limited by this factor. For thinner electrodes and at low discharge rates, the external mass transfer can be neglected since the concentration of hydroxide is large (6 MKOH). However, at higher discharge rates for thick electrodes, this external mass transfer becomes rate limiting. The deviation of the model simulation from the experimental results at large alloy weights arises because of this. For 0.65 g of alloy weight at high discharge rates the deviation is even more pronounced.

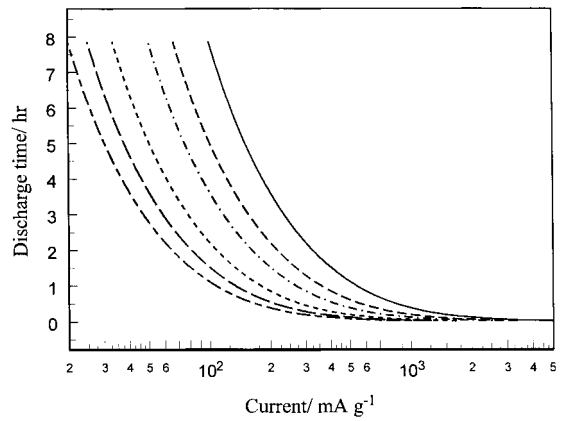

Fig. 11. Model predictions for the discharge time at different discharge rates. Key: (——) 0.040, (– – – –) 0.060, (·—·—·) 0.080, (- - - -) 0.120, (— — — —) 0.160 and (- – - –) 0.200 g.

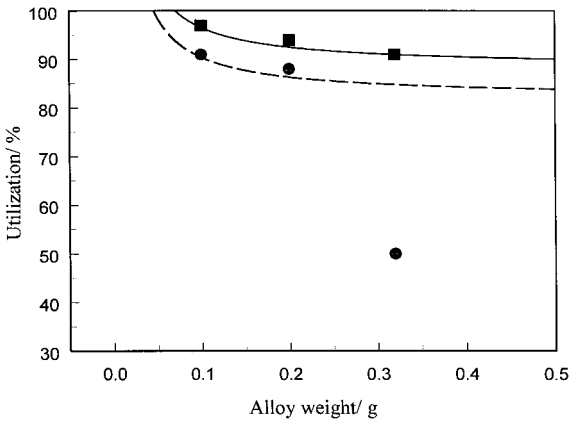

Fig. 12. Electrode utilization as a function of alloy weight for two different discharge rates. The lines represent the model simulations and the points the experimental data. The solid square corresponds to a 0.1 *C* rate and the solid circle corresponds to a 0.2 *C* rate. Key: (——) 0.1 *C* and (— — —) 0.2 *C*.

The effect of the alloy weight on the utilization is more pronounced at high discharge rate (0.2 *C*). For example, the electrode utilization is only about 10% at 0.2 *C* rate compared with 70% at 0.1 *C* rate for 0.65 g of the active electrode material. As mentioned before, increasing the alloy weight results in a thicker electrode. At high discharge rates, accessing the active material (OH^- ions) in the interior of the electrode becomes prohibitively difficult. Under such conditions, the hydrogen in the particles closer to the current collector are depleted fast. This results in a very low utilization as seen in Fig. 12. It is pertinent to note that the effect of alloy weight is analogous to that of PTFE content as seen in Fig. 10.

Finally, we examine the effects of particle size on the power and energy density of the hydride electrode. Figure 13 shows a Ragone plot for different particle radius. The power provided here is an average value over the course of discharge. Hence, each point on this plot is obtained by carrying out a constant-current discharge at a particular discharge rate to a cut-off potential of −0.6 V. The energy and the average power available during discharge were then calculated. At low current densities, the energy density approaches a theoretical limit, which is a function of the open-circuit potential. The energy density increases slightly due to the decrease in the particle size. However, a more pronounced effect is seen on the power density of the alloy. A smaller particle reduces the time taken by hydrogen to reach the surface. Hence this increases the power density significantly. However, reducing the particle size also results in exposing more area of the active material to the electrolyte. This would result in enhanced corrosion of the alloy. Thus, there exists a trade-off between the maximum realizable power density (by using smaller particles) and a long cycle life of the alloy.

5. Conclusions

$LaNi_{4.27}Sn_{0.24}$ electrodes were characterized using electrochemical techniques at different alloy weights and binder contents. EIS combined with an equivalent circuit is used to determine different electrode resistances. Increase in alloy weight has no effect on the ohmic resistances of the electrode. For electrodes containing a large amount of alloy weight (0.65 g), the total resistance is controlled by the ohmic resistance at a wide range of state of charge. Similarly, at a low SOC the polarization resistance is found to be independent of SOC. However, as the hydrogen content increases the polarization resistance also increases due to changes from the α to the β phases and also due to variations in the alloy electroactive area. Since the interfacial area determines the polarization resistance an increase in the alloy weight reduces R_p and lowers the total resistance. This, gives rise the need to normalize the equilibrium reaction rates based on the total alloy weight in the electrode. Finally, the role of different amounts of PTFE on the performance of the hydride electrode has been studied. It is seen that 5% by weight of PTFE represents the optimum value of the binder for both higher reaction rates and better utilization of the hydride electrode. Using lower PTFE contents increases the particle–particle resistance due to poor contact among various particles in the alloy. Adding more PTFE results in reducing the active material in the alloy and thereby reducing the utilization of the electrode. Also, increase of the binder content results in increase of the resistance since the binder acts as an insulator. The electrode utilization decreases on increasing the binder content and the electrode weight. The model simulations predict a lowering of the utilization with increase in the electrode weight. The electrode thickness plays a crucial role in this context. The effect of particle size on the energy and power density of the electrode was studied using a Ragone plot.

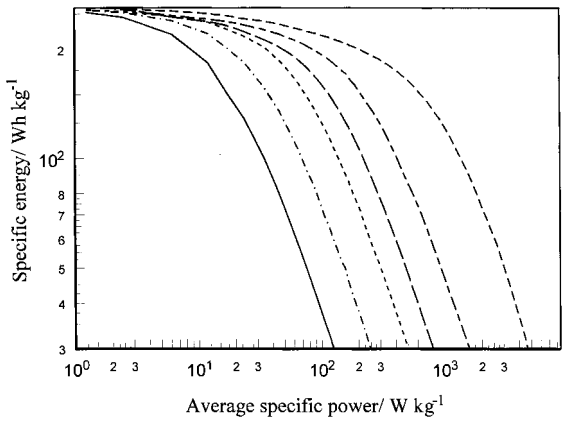

Fig. 13. Ragone plot for the $LaNi_{4.27}Sn_{0.24}$ electrode showing the effect of particle size. Key: (——) 45, (—·—·) 30, (- - - - -) 20, (— — —) 15, (– — – —) 10 and (– – – –) 5 μm.

Acknowledgements

Financial support by the Exploratory Technology Research (ETR) Program, which is supported by the Office of Transportation Technologies (OTT) of the US Department of Energy (DOE), subcontract 4 614 610 is acknowledged gratefully.

References

[1] T. H. Fuller and J. Newman, 'Modern Aspects of Electrochemistry', Vol. 27, edited by R. E. White, J. O'M. Bockris, B. E. Conway (Plenum Press, New York, 1993), p. 359.
[2] G. Zheng, B. N. Popov and R. E. White, *J. Electrochem. Soc.* **143** (1996) 435.
[3] G. Zheng, B. N. Popov and R. E. White, *J. Electrochem. Soc.* **143** (1996) 834.
[4] N. Kuriyama, T. Sakai, H. Miyamura. I. Uehara and H. Ishikawa, *J. Alloys Comp.* **202** (1993) 183.
[5] N. Kuriyama, T. Sakai, H. Miyamura, I. Uehara and H. Ishikawa, *J. Alloys Comp.* **192** (1993) 161.
[6] N. Kuriyama, T. Sakai, H. Miyamura, I, Uehara and H. Ishikawa, *J. Electrochem. Soc.* **139** (1992) L72.
[7] W. Zhang, M. P. S. Kumar, and S. Srinivasan, *J. Electrochem. Soc.* **142** (1995) 2935.
[8] P. Agarwal, M. E. Orazem, A. Hiser, 'Hydrogen Storage Materials, Batteries, and Electrochemistry', PV 92–5, edited by D. A. Corrigan and S. Srinivasan (The Elec-

trochemical Society Proceedings Series, Pennington, NJ, 1992), p. 120.
[9] B. N. Popov, G. Zheng and R. E. White, *J. Appl. Electrochem.* **26** (1996) 603.
[10] G. Zheng, B. N. Popov and R. E. White, *J. Electrochem. Soc.* **142** (1995) 2695.
[11] A. Zuettel, F. Meli and L. Schlapbach, *J. Alloys Comp.* **221** (1995) 207.
[12] B. S. Haran, B. N. Popov and R. E. White, *J. Electrochem. Soc.* **145** (1998) 4082.
[13] J. R. Macdonald (ed.), 'Impedance Spectroscopy, Emphasizing Solid Materials' (J. Wiley & Sons, New York, 1987).
[14] W. Tobias and L. G. Austin, *Electrochim. Acta* **14** (1965) 639.